

DSCC2017-5217

THE DEVELOPMENT OF HIGH SPEED VIRTUAL MILLING TEST

Akos Miklos*
Denes Takacs

MTA-BME Research Group on Dynamics of Machines and Vehicles
Budapest University of Technology and Economics
Budapest, Hungary
Email: miklosa@mm.bme.hu, takacs@mm.bme.hu

Richard Wohlfart
Gabor Porempovics
Tamas G. Molnar
Daniel Bachrathy

Department of Applied Mechanics
Budapest University of Technology and Economics
Budapest, Hungary
Email: wohl@mm.bme.hu, poremg@mm.bme.hu,
molnar@mm.bme.hu, bachrathy@mm.bme.hu

Andras Toth

Department of Manufacturing Science and Engineering
Budapest University of Technology and Economics
Budapest, Hungary
Email: toth@manuf.bme.hu

Gabor Stepan

Department of Applied Mechanics
Budapest University of Technology and Economics
Budapest, Hungary
Email: stepan@mm.bme.hu

ABSTRACT

The concept of a hardware-in-the-loop experiment for high speed milling is introduced in this paper. The tool-workpiece interaction is virtually implemented in the experiment while the milling machine with the spindle is used as real element. In this paper, the basic components of the experiment are presented, namely, a contactless displacement sensor, a computational algorithm of the cutting force and a contactless electromagnetic actuator are discussed. Experiments on the prototype of the electromagnetic actuator are also shown to illustrate the potential of the concept. A feasibility study of the hardware-in-the-loop experiment is given, where the effect of the time delay included in the experiment is investigated.

INTRODUCTION

One of the most intricate phenomenon of milling is the chatter vibration, which usually leads to improper surface quality or

in worst case it can also lead to the damage of the milling machine. Theoretical analyses of the models of high speed milling processes aim to predict both the linear stability limits of cutting and the so-called unsafe parameter domains in the linearly stable regions where chatter may still occur with certain probability. The industrial applications of these theoretical results are still limited by the availability of extensive laboratory tests required for the validation of the models in case of various working conditions and tool geometries, and also to explore the range of uncertainties of certain parameters. The cost of these tests could be reduced substantially by so-called hardware-in-the-loop (HIL) experiments in which the real tool-workpiece interaction is emulated.

The reliability of HIL experiments strongly depends on the applied sampling frequency that can be used during the simulation and emulation of the cutting forces. For example, the stick-and-slip phenomenon is deeply analyzed in [1], where the asymmetric non-linearity of the Stribeck contact force is similar to that of the cutting force. It is shown in [1] that the HIL experi-

*Address all correspondence to this author.

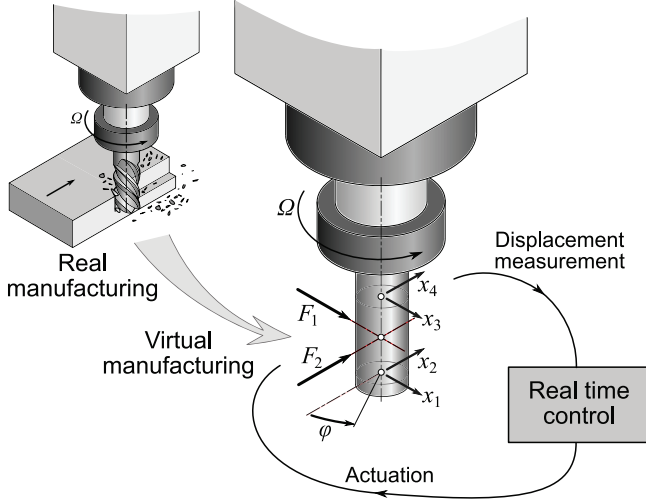


FIGURE 1. THE CONCEPT OF THE HIL EXPERIMENT.

ments do not provide conservative estimates if the sampling time is larger than a critical value, namely large time delay in the loop can also stabilize the system in certain parameter ranges.

The goal of this research is the development of a HIL experiments for high-speed milling processes, which can also be considered as semi-virtual machining. The machine tool structure together with the tool, the spindle and its bearings are there physically, while the forces generated by the cutting process are calculated by real time target computer and they are emulated by actuators. The loop is closed by means of the displacement measurement of the tool.

In this paper, the concept of a HIL experiment is in focus with special attention to the bottlenecks of the semi-virtual manufacturing concept. Linear stability charts of the real and the semi-virtual manufacturing are compared to identify the requirements for the sampling time of the HIL test. After this, we deal with a laser sensor and an electromagnetic actuator that are developed and tested by the research group in simple experiments. The computational algorithm of the cutting force is also presented.

CONCEPT OF THE HIL TEST

The concept of the HIL experimental setup is shown in Fig. 1. Instead of having the real milling tool with its contact with the workpiece, a dummy tool is fixed into the main spindle. The position of this dummy tool is measured in radial directions at two different cross-sections. The angular position of the tool about the rotational axis is determined by the rotational encoder of the spindle. The torsional and longitudinal vibrations of the spindle are not considered in the experiment since we focus on the cases when the chatter vibration corresponds to the bending modes of the tool and the spindle, which are related to lower

natural frequencies than the torsional, and especially longitudinal ones. Since the real contact of the tool and the workpiece is eliminated, the resultant cutting force (i.e. the contact force) has to be emulated. The cutting force is calculated by means of a real time computational algorithm using the measured positions of the dummy tool. In the computation algorithm complex virtual tools, workpiece geometries and material properties can be considered.

Clearly, the real contact dynamics between the tool and the workpiece is more complex than the one that can be emulated by an actuator. Due to technical reasons it is impossible to generate the exact distributed force system acting on the tool in case of real manufacturing, but the generation of the radial component of the resultant cutting force seems to be a satisfactory solution from the viewpoint of checking chatter.

Three essential technical problems can be emphasized in connection with the HIL experiment:

- the contactless displacement measurement of the rotating tool,
- the real time computation of the cutting force,
- the contactless actuation of the cutting force.

Solutions are presented in the following subsections of the paper for all these problems. First of all, a theoretical study is performed on the linear stability of the HIL experiment.

STABILITY AND CRITICAL SAMPLING TIME OF THE HIL EXPERIMENT

It is a general requirement for HIL experiments that they match the emulated process in terms of dynamics and stability. In case of milling, the HIL test must be able to accurately predict the stability of metal cutting and anticipate the loss of stability that leads to machine tool vibrations. While an actual milling operation is a continuous-time process, the HIL experiment uses sampled input and output signals. Hereinafter, we analyze the effect of the sampling time on the stability of the emulated milling operation by making comparison with the actual continuous-time process. We formulate the governing equations of milling and conduct stability analysis both with and without the effects of sampling.

The differential equation governing the dynamics of milling processes is of the form [2–4]

$$\ddot{\mathbf{q}}(t) + \mathbf{C}_m \dot{\mathbf{q}}(t) + \mathbf{K}_m \mathbf{q}(t) = \mathbf{W}(t) (\mathbf{q}(t - \tau) - \mathbf{q}(t)), \quad (1)$$

where the left-hand side is a multiple-degrees-of-freedom model that describes the dynamic behavior of the machining system (including the spindle, the tool holder, the tool, and the workpiece). Vector \mathbf{q} consists of the modal coordinates associated with the relative motion between tool and workpiece, whereas \mathbf{C}_m and \mathbf{K}_m

are modal matrices related to the damping ratios and natural frequencies of the modeled vibration modes. The right-hand side of Eqn. (1) represents the variation of the cutting force acting on the mill that depends on the actual tool position associated with $\mathbf{q}(t)$ and on the tool position at the previous cut related to $\mathbf{q}(t - \tau)$. Accordingly, τ denotes the time that elapses between the subsequent cuts – it is the tooth-passing period that is inversely related to the spindle speed Ω and the number N of cutting teeth: $\tau = 1/(N\Omega)$. The coefficient $\mathbf{W}(t) = \mathbf{W}(t + \tau)$ is τ -periodic as the direction of the cutting force changes periodically and the teeth of the mill enter and exit the workpiece material repeatedly. The periodic coefficient $\mathbf{W}(t)$ is linearly proportional to the axial depth of cut a_p and depends on the number of cutting teeth, the tool geometry, the feed per tooth, and the cutting force characteristics (see [2, 4, 5]). Note that Eqn. (1) is a delay differential equation with time-periodic coefficient, where τ is also called as regenerative delay.

The dynamic system on the left-hand side of Eqn. (1) is physically present in the HIL experiment, whereas the cutting force variation on right-hand side is emulated by the control loop. This virtual cutting force is calculated from measured tool positions sampled with sampling time Δt , and it is held constant by a zero-order-hold along each sampling period. Between the k -th and $(k + 1)$ -th sampling time, the $(k - 1)$ -th position data $\mathbf{q}(t_{k-1})$ can be used as actual position (instead of $\mathbf{q}(t)$) and the $(k - r)$ -th data $\mathbf{q}(t_{k-r})$ can be used as position at the previous cut (instead of $\mathbf{q}(t - \tau)$), where $k \in \mathbb{N}$, $t_k = k\Delta t$, $r = \text{int}(\tau/\Delta t)$. Since the dynamics of the electromagnetic actuator, which is planned to be used in the HIL test, is much faster than the dynamics of the system of the tool and the spindle, it is not considered in our calculation. Therefore, the governing equation in the case of the HIL experiment becomes

$$\ddot{\mathbf{q}}(t) + \mathbf{C}_m \dot{\mathbf{q}}(t) + \mathbf{K}_m \mathbf{q}(t) = \mathbf{W}_k (\mathbf{q}(t_{k-r}) - \mathbf{q}(t_{k-1})), \quad (2)$$

$$t \in [t_k, t_{k+1}),$$

where $\mathbf{W}_k = \int_{t_k}^{t_{k+1}} \mathbf{W}(t) dt / \Delta t$ is the constant approximation of $\mathbf{W}(t)$ along $[t_k, t_{k+1})$. Note that due to the sample-and-hold unit, the right-hand side is piecewise constant, and a short time delay appears in the governing equation in addition to the regenerative delay as the delayed position $\mathbf{q}(t_{k-1})$ is used instead of the actual position $\mathbf{q}(t)$. The additional delay arising in sampled-data systems is in fact time-periodic and varies between Δt and $2\Delta t$ in each sampling period, see [6, 7]. Moreover, the regenerative delay τ in $\mathbf{q}(t - \tau)$ is also modified and is resolved by integer (r) multiples of the sampling period.

The short delay introduced by sampling may interact with the large regenerative delay. If the sampling time is not small enough, the interplay between the two delays may affect the stability of the virtual milling process and the onset of machine tool vibrations. In order to make sure that the sampling time 0.01

ms is sufficiently small for accurate stability prediction, we conducted stability analysis for Eqns. (1) and (2) using the semi-discretization technique [3]. We analyzed stability for a representative case study assuming a particular set of cutting parameters. We investigated an up-milling process with 25% radial immersion using a straight-fluted tool with two cutting teeth. The modal matrices \mathbf{C}_m and \mathbf{K}_m were obtained from fitting a six-degrees-of-freedom model to the frequency response function measured by impact hammer tests on an actual three-axis milling machine. In order to calculate the periodic coefficient $\mathbf{W}(t)$, we used the well-known three-quarter rule [4] as cutting force characteristics with linearized tangential and radial cutting force coefficients $800 \times 10^6 \text{ N/m}^2$ and $300 \times 10^6 \text{ N/m}^2$, respectively. For details on the computation of the periodic coefficient, the reader is referred to Chapter 5.2 of [3].

We investigated the spindle speed range $3 \leq \Omega \leq 30 \text{ krpm}$, which corresponds to regenerative delays $10 \geq \tau \geq 1 \text{ ms}$. During semi-discretization, the discretization step was the sampling time 0.01 ms itself, whereby the tooth-passing period τ was resolved by 1000..100 intervals. Since such large period resolutions significantly increase the computational time of numerical stability analysis, we used the multi-dimensional bisection method (for more details please see [8]) to speed up the computations. This method reduces the number of computations since it focuses the computations only around the stability boundaries without computing the eigenvalues of the system on a fine mesh that completely covers the interested parameter space. For the achieved resolution of the boundaries, the computation time was reduced to ca. 17.5% by means of this method.

The results are summarized by the stability chart shown in Fig. 2. In this diagram, the boundaries of linear stability are depicted in the plane of the spindle speed Ω and the axial depth of cut a_p . The diagram identifies the technological parameters associated with stable stationary cutting (grey shaded region) from those accompanied by machine tool vibrations (white region). The stability boundaries of the continuous-time system (1) are indicated by thick black lines, while solid red lines show the stability boundaries of the HIL experiment (2) with sampling period 0.01 ms. It can be seen that the stability boundaries obtained with and without considering sampling lie close to each other, which implies that the effect of sampling is negligible compared to other effects such as parameter uncertainties and unmodeled dynamics.

This verifies that the sampling period 0.01 ms is sufficiently small for accurate stability prediction. In order to estimate how safe using 0.01 ms is, the stability boundaries corresponding to 0.02 ms, 0.05 ms, and 0.1 ms sampling times are also shown by green, blue, and purple thin lines, respectively. The figure shows that the effect of sampling becomes more pronounced with increasing sampling time, which was also observed by other HIL experiments in the literature [1]. We can conclude that although the sampling time 0.01 ms is sufficient for emulating the dynam-

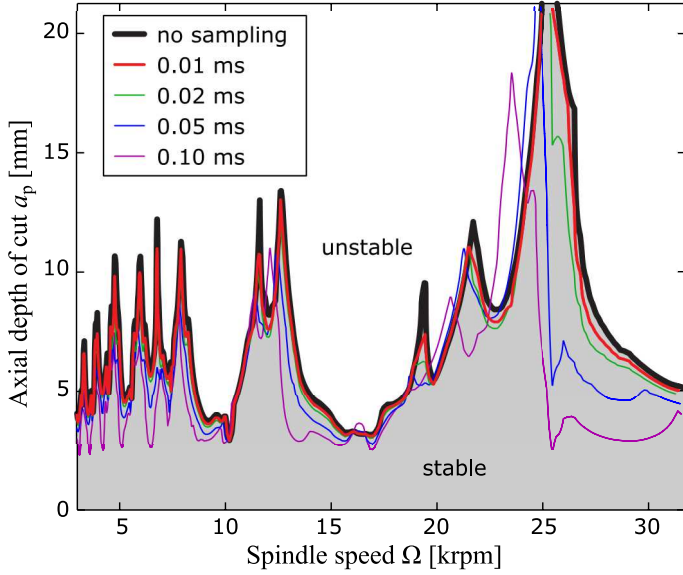


FIGURE 2. STABILITY CHART ILLUSTRATING THE EFFECT OF THE SAMPLING TIME ON THE STABILITY OF VIRTUAL MILLING PROCESSES.

ics of milling, it is also necessary to use such small sampling periods.

CONTACTLESS DISPLACEMENT MEASUREMENT

To measure the radial position of the dummy tool, displacement sensors are needed. The contactless measurement is a common wish in the field of rotor dynamics and machine tool vibration detection. For example, to construct the theoretical stability charts of milling processes frequency response functions (FRFs) are required. FRFs of the tool side are measured with impact hammers and accelerometers attached to the non-rotating tool tip. However, it is well known, that stiffness and damping parameters of angular contact bearings vary with the angular speed, and the gyroscopic effect can also be relevant at high rotational speed (see [9]). To identify the speed varying dynamics of the spindle, FRFs has to be measured at non-zero spindle speed.

Contactless measurement could also be very useful for the detection of chatter vibrations that may arise during the machining. Nowadays, accelerometers attached to non-rotating parts of the machine or to the workpiece, microphones or force transducers are used to identify the chatter and the linear stability boundaries of the milling process in real time. But all the mentioned cases enable indirect identification of the chatter, and are much more uncertain than the direct displacement measurement of the milling tool could be.

A commonly used contactless measurement device is the Laser-Doppler vibrometer that measures the velocity of the ob-

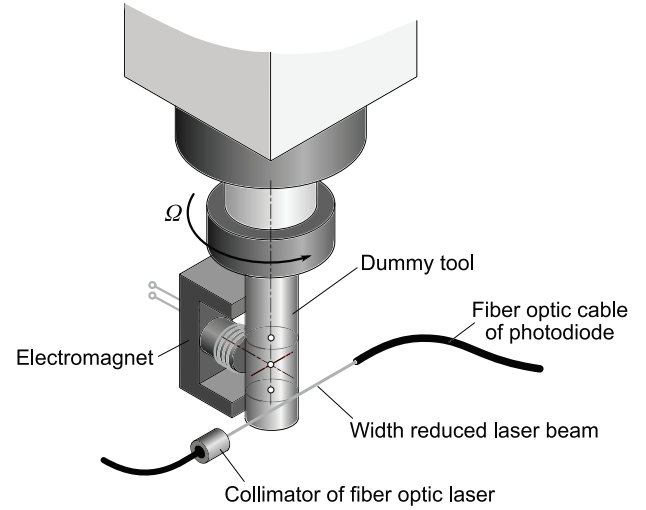


FIGURE 3. SCHEMATIC ILLUSTRATION OF THE FOTONIC BEAM REDUCTION (FBR) SENSOR AND THE ELECTROMAGNET IN THE ACTUATOR PROTOTYPE.

ject in one direction. In the HIL experiment, accurate displacement measurement is demanded in wide frequency domain in order to calculate the resultant cutting force, thus, Laser-Doppler vibrometers are not useful for this task. There are reflective laser based displacement sensors on the market with different measuring range and resolution, but their frequency bandwidth and resolution are limited.

In order to exploit all the advantageous properties of laser based sensors in our HIL test, a sensor was constructed with very high resolution and frequency bandwidth. The basic idea of the developed FOTONIC BEAM REDUCTION (FBR) sensor is illustrated in Fig. 3. A laser beam is tangentially directed to the dummy tool and the intensity of the laser beam is measured by a photodiode at the other side of the tool. If the tool moves in the transverse direction of the laser beam, the laser beam fades in/out the width of the laser beam received by the photodiode is modulated and the measured intensity increases/decreases. Namely, light intensity is proportional with the displacement of the tool. Similar devices are also applied for exact tool geometry measurement and failure detection. But here, due to the large time-varying magnetic field, which is generated by the actuator, the isolation of the FBR sensor is carried out using fiber optic elements.

In Fig. 4 the performance of the FBR sensor is illustrated. The displacement of the dummy tool was measured by the FBR sensor meanwhile the tool was moved with $1 \mu\text{m}$ steps. The RMS noise level is below 100 nm . The characteristics of the sensor is plotted in bottom panel. The measuring range is cc. 0.2 mm . The most sensitive range of the sensor corresponds to the most linear domain, where the sensitivity is around $48 \text{ mV}/\mu\text{m}$. The frequency bandwidth of the sensor is 500 kHz .

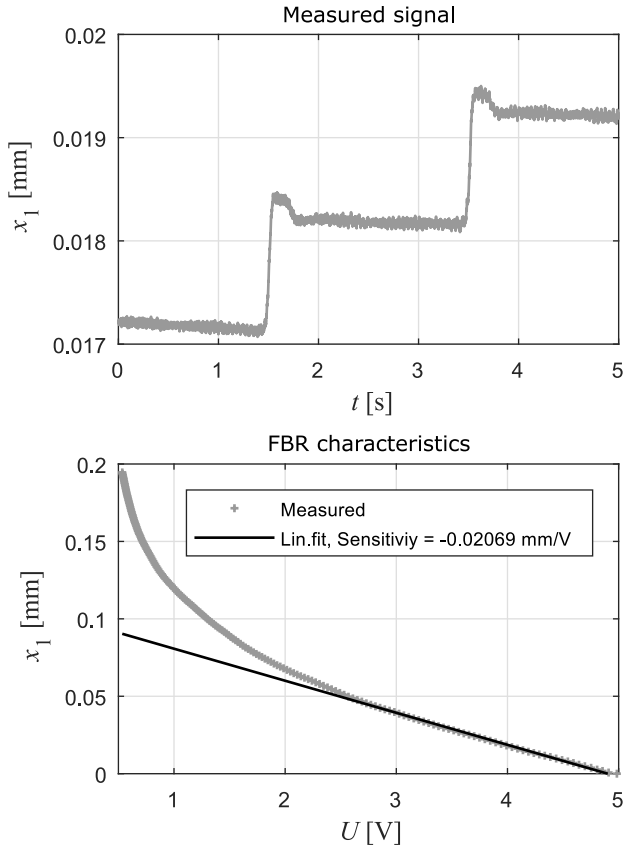


FIGURE 4. DISPLACEMENT OF THE TOOL MEASURED BY THE FBR SENSOR AND THE DETERMINED CHARACTERISTICS OF THE FBR SENSOR.

REAL TIME CALCULATION

In the HIL test, the cutting force is emulated on the dummy tool with the help of an actuator. The actual cutting force can be calculated based on the algorithm given in [5], where the linear stability analysis of milling is investigated for different tool geometries and technological parameters.

Computation algorithm

In the experiment, we intend to emulate the deviation of the cutting force from the theoretically determined stationary force that also generates the stationary vibration of the tool. This limitation is required because the developed actuator cannot generate large enough forces since the wide frequency bandwidth was rather kept in focus during the design. In the algorithm, when the cutting force is calculated, we consider that the non-stationary part of the cutting force depends linearly on the chip thickness, which is determined based on the actual position of the dummy tool. Namely, we measure

- the rotational position $\varphi(t)$ of the spindle;
- the transverse positions of two cross sections of the dummy tool via $x_1(t)$, $x_2(t)$, $x_3(t)$ and $x_4(t)$.

The computational algorithm is required to determine the cutting force and corresponding output signals for the actuator. In our final actuator, four electromagnets will generate the components F_1 and F_2 of the in-plane force (see Fig. 1). Namely, the desired current values $i_1(t)$, $i_2(t)$, $i_3(t)$ and $i_4(t)$ of the coils have to be provided.

Based on the sampling frequency f of the real target computer, the sampling time $\Delta t = \frac{1}{f}$ can be introduced and the time can be quantized as $t_k = k\Delta t$, $k = 0, 1, 2, \dots$. Namely, the input/output signals are discretized in time:

$$x_{i,k} := x_i(t_k), \quad \varphi_k := \varphi(t_k) \quad i_{j,k} := i_j(t_k). \quad (3)$$

By means of Eqn. (2), the cutting force components can be calculated as:

$$F_{l,k+1} = \sum_{i=1}^4 \tilde{\mathbf{w}}_{lir}^T \mathbf{x}_{i,k} \quad \text{for } l = 1, 2, \quad (4)$$

where

$$\mathbf{x}_{i,k} = [x_{i,k} \ x_{i,k-n_\tau} \ x_{i,k-2n_\tau} \ \dots \ x_{i,k-Nn_\tau}]^T, \quad i = 1, 2, 3, 4, \quad (5)$$

contains the actual and the past values of the displacements. The value of n_τ can be calculated as

$$n_\tau = \text{int} \left(\frac{T}{N_t \Delta t} \right), \quad \text{where } N_t \leq T/\Delta t \Rightarrow 1 \leq n_\tau. \quad (6)$$

The time period $T = 2\pi/\Omega$ corresponds to one revolution of the spindle, where Ω is the angular speed. Thus, N_t specifies how many former values of measured displacement signals are used in the calculation of the cutting force. The larger N_t is, the more precise the consideration of the regenerative effect is. Hence, N_t can be thought of as the resolution of the time domain.

The notation $\tilde{\mathbf{w}}_{lir}$ in Eqn. (4) refers to the constant vectors:

$$\tilde{\mathbf{w}}_{lir} = [w_{lir1} \ w_{lir2} \ \dots \ w_{lir(N_t+1)}]^T \quad (7)$$

that can be obtained by a specific rearrangement of the elements of the \mathbf{W}_k matrices in Eqn. (2). The index r depends on the angular position of the spindle, and it can be calculated as

$$r = \text{int} \left(\frac{\text{mod}(\varphi_k, 2\pi)}{n_\varphi \Delta \varphi} \right) + 1, \quad (8)$$

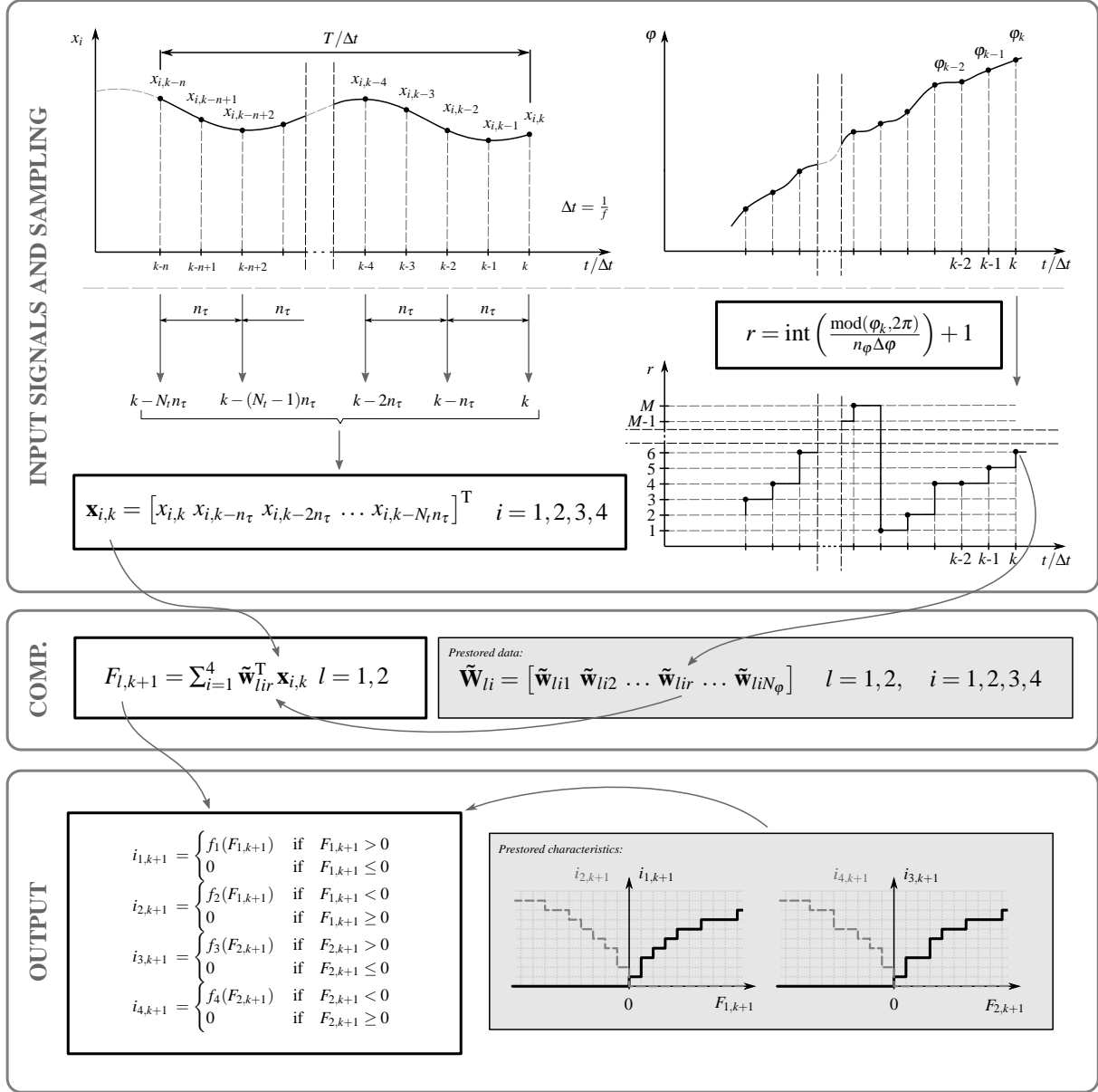


FIGURE 5. COMPUTATIONAL ALGORITHM TO CALCULATE CUTTING FORCE.

where

$$n_\varphi = \frac{2\pi}{N_\varphi \Delta \varphi}, \quad \text{where } N_\varphi \leq 2\pi/\Delta \varphi \Rightarrow 1 \leq n_\varphi. \quad (9)$$

The resolution parameter N_φ determines how many rotational positions of the tool are differentiated in the computation algorithm. The larger N_φ is, the more precise the calculation is.

Vectors $\tilde{\mathbf{w}}_{li}$ can be arranged in the matrices:

$$\tilde{\mathbf{W}}_{li} = [\tilde{\mathbf{w}}_{li1} \ \tilde{\mathbf{w}}_{li2} \ \dots \ \tilde{\mathbf{w}}_{liM}] , \quad l = 1, 2, \quad i = 1, 2, 3, 4, \quad (10)$$

which can be preprocessed for a given milling tool geometry and cutting parameters, and they can be stored in the memory of the real target.

Based on the calculated cutting force components $F_{l,k+1}$, the desired currents of the electromagnet coils can be determined

TABLE 1. NUMBER AND TYPES VARIABLES

Variable	Type	Number of stored values
x_i	16 bit	$4 \times T/\Delta t$
φ	10 bit	1
\mathbf{x}_i	16 bit	$4 \times (N_t + 1)$
$\tilde{\mathbf{W}}_{li}$	16 bit	$8 \times (N_t + 1) \times N_\varphi$
F_l	16 bit	2
f_j	16 bit	4×256

TABLE 2. NUMBER OF COMPUTATIONAL OPERATIONS

Formula	Type	Number of operations
Eqn. (4)	Multiplication	$2 \times 4 \times (N_t + 1)$
	Addition	$2 \times (4 \times (N_t + 1) + 4)$

TABLE 3. MEMORY STORAGE AND NUMBER OF COMPUTATIONAL OPERATIONS FOR DIFFERENT SETUPS

Setup	$T/\Delta t$	N_t	N_φ	Mem.(kbit)	No.comp.oper.
Min.	200	100	128	1675	1684
Sat.	400	200	256	6626	3224
Ideal	400	400	512	26332	6424

by means of the characteristics f_j ($j = 1, 2, 3, 4$) of the electromagnets, which are determined via a calibration process. The computation algorithm described above is summarized in Fig. 5, where these characteristics are also illustrated.

Computation effort

As it was established by the stability analysis, an acceptable sampling frequency for the HIL test corresponds to 100 kHz. This means that $10\mu s$ is available to generate the cutting force based on the actually measured displacements of the tool, which is a very hard requirement against the real target computer. To make this requirement more illustrative, the computational efforts required by the algorithm are detailed in this section.

The variables used in the algorithm are summarized in Tab. 1, where their type and sizes are also given. Table 2 contains the numbers of computational operations. As it can be seen, the memory usage and the numbers of the operations depend on the time period T , on the sampling time Δt and on the resolutions N_t and N_φ . The larger N_t and N_φ are, the more accurate the computation algorithm is, and consequently, the higher the required computational effort is.

Based on our theoretical studies, minimal, satisfactory and ideal resolutions are determined. The corresponding memory usage and numbers of the computational operations are calculated in Tab. 3. Due to the fact that the numbers of operations are high and the available computation time is very small, linear processors are not applicable to realize the HIL experiment. However, the main formula of our computation in Eqn. (4) can be split and it can carry out using parallel computation technique. Thus, Field-Programmable Gate Array (FPGA) technology can be beneficial but the memory usage of the computation is the bottle neck. Nevertheless, the computational algorithm has been compiled with the ideal resolutions on NI PXIe architecture using Xilinx Kintex[®]7 XC7K410T FPGA chip.

ACTUATOR

The excitation of the rotating spindle is another difficult problem even if a simple FRF has to be identified. Electrodynamic exciters can be attached to a rotating tool with the help of bearing that transfers the force from the exciter to the tool but the additional dynamics of the bearing can modify the original dynamics of the tool-spindle system. Thus, a contactless excitation of the tool is desired. Electrodynamic actuators are already developed for the contactless excitation of milling spindles in [10–13].

Here we present a prototype of an actuator having different electromagnet orientations and locations (see Fig. 3). Our design focuses on high speed milling processes, correspondingly, the frequency bandwidth of the actuator reaches 100 kHz and it also works for high rotational speeds. Advanced FPGA based current control with 1 MHz switching frequency is under the design stage for the electromagnetic coils.

Test of the prototype

To test the concept of the actuator, a prototype is designed and built with a single electromagnet and FBR sensor, see Fig. 6. The diameter of the dummy tool is 11 mm, and the air-gap between the tool and the E-shape magnetic core is 0.1 mm.

Without having the current control of the electromagnet, we managed to test the power electronics. Namely, the coil is switched into on/off states by a function generator using narrow impulses in the control signal. In the experiments, the displacement of the dummy tool is measured and the generated force of actuator is determined indirectly using the FRF of the dummy tool. The FRF is identified in a classical way, namely, modal hammer and the FBR sensor are used.

Figure 7 shows the displacement of the dummy tool and the calculated force for the case when the coil is switched on for

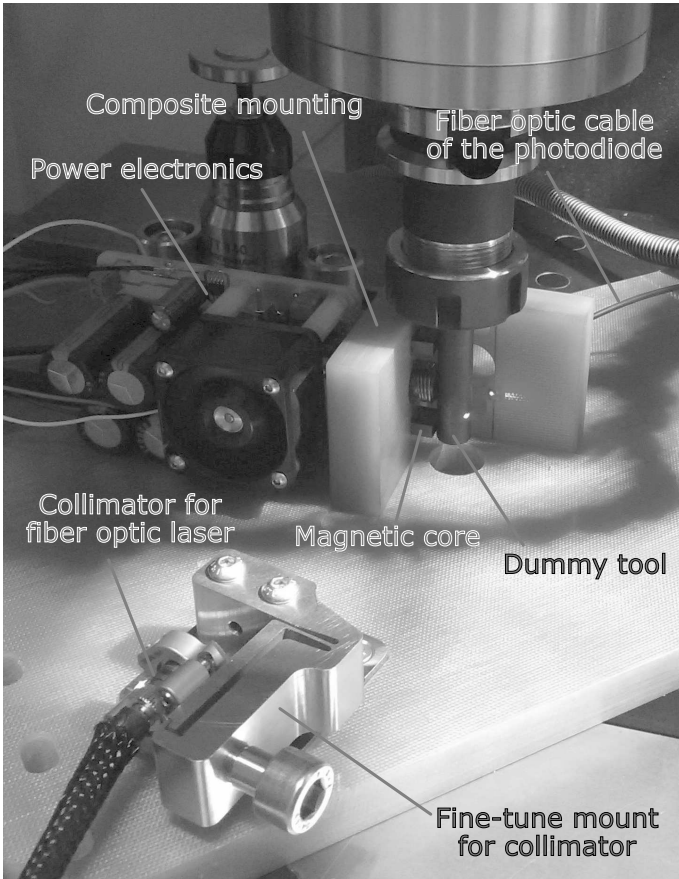


FIGURE 6. THE PROTOTYPE OF THE ACTUATOR.

5 ms. Gray curves refer to the measured and calculated values while black curves represent the mean values of the signals determined by moving average. A high frequency vibration of the tool appears as a result of the transient force excitation. This vibration also makes the calculated force signal noisy since the FRF is not accurate in that frequency domain. It can also be observed that the deformation reaches its maximum after a short time since the magnetic field saturates in the magnetic core and/or in the dummy tool. As a result of this saturation the current in the coil run up to higher values speeding up the heat generation in the electric circuit without the further increase of the force magnitude. Namely, the maximum achievable force that can be generated by the prototype actuator is about 12 N.

Figure 8 illustrates the case when 30 μ s wide impulses are used to switched on the coil. 1000 impulses are sent to the power electronics with 10 kHz base frequency. As a result, the tool deformation is built up and it is hold for 0.1 s without generating extreme current in the coil.

The same number of impulses are used as control signal in Fig. 9 but the rotational speed of the spindle is set to 30000 rpm.

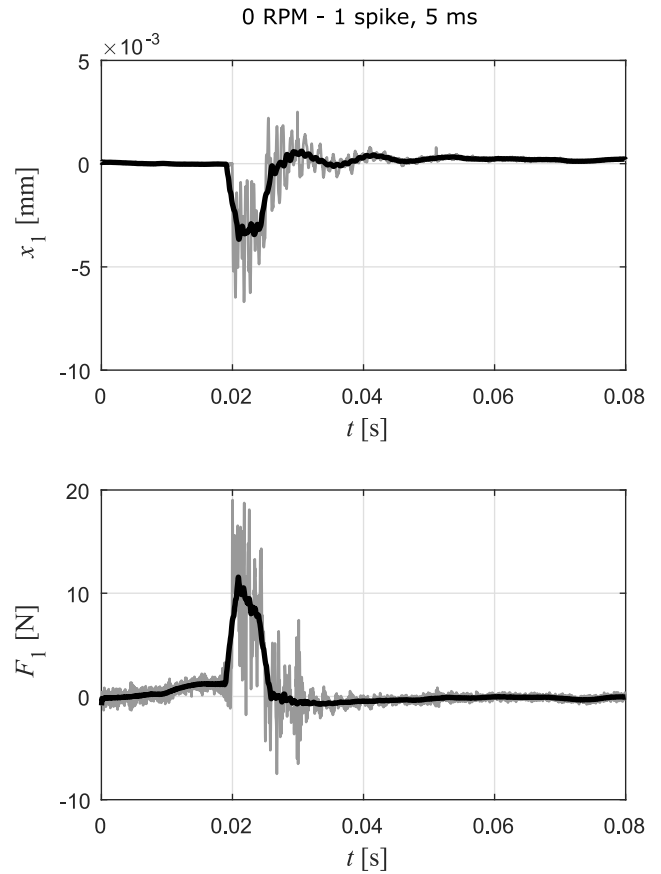


FIGURE 7. DISPLACEMENT GENERATED BY 5 ms LONG IMPULSE AND THE CALCULATED FORCE (0 RPM).

The run-out (cc. 23 μ m) of the dummy tool can be clearly identified in the measured signal. The 1000 impulses are repeatedly sent to the power electronics with 1 s time period, which generates the same displacement of the dummy tool as in Fig. 8. This test confirms the concept of the actuator, namely the applied magnetic cores support the emulation of the cutting force even at high rotational speed.

CONCLUSION

The concept of virtual milling and its difficult-to-handle aspects were introduced in this paper. A contactless laser sensor (referred to as Fotonic Beam Reduction (FBR) sensor) was developed to measure the displacements of the rotating tool with high accuracy and with high frequency bandwidth even in the present of time-varying strong magnetic field. The computation algorithm of the virtual cutting force was given in details with special attention to the required computation efforts and the extremely short sampling time. A feasibility study of the HIL

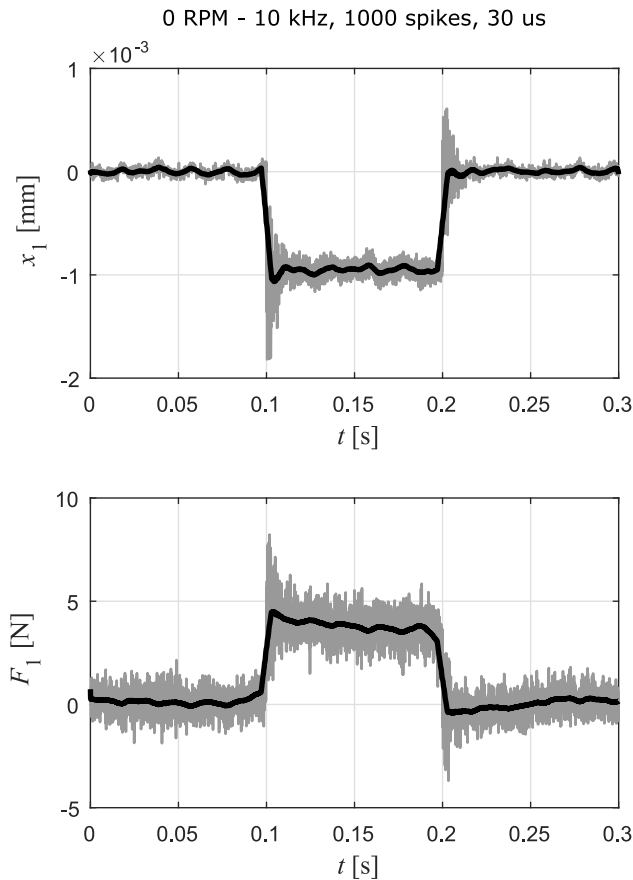


FIGURE 8. DISPLACEMENT GENERATED BY MANY $30 \mu\text{s}$ LONG IMPULSES AND THE CALCULATED FORCE (0 RPM).

experiment was carried out by comparing the linear stability of the real and virtual milling processes. It was shown that in case of 100 kHz sampling frequency the virtual manufacturing can provide useful information about the linear stability boundaries, namely, the stability chart is well approximated in the HIL experiment. The prototype of the contactless electromagnetic actuator was presented in the paper. Simple experiments proved that the actuator can generate suddenly changing cutting forces with good resolution but with limited amplitude.

Although the final assembly of the HIL test and the first virtual machining experiments are the tasks of future work, the practical experiences on the three intricate parts of HIL test suggest promising results.

ACKNOWLEDGMENT

The research leading to these results has received funding from the European Research Council under the European Unions Seventh Framework Programme (FP/2007-2013) / ERC

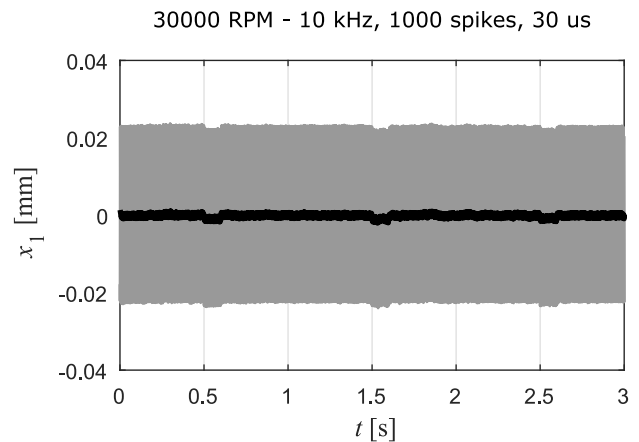


FIGURE 9. DISPLACEMENT GENERATED BY MANY $30 \mu\text{s}$ LONG IMPULSES AND THE CALCULATED FORCE (30000 RPM).

Advanced Grant Agreement n. 340889.

REFERENCES

- [1] Veraszto, Z., and Stepan, G., 2017. "Nonlinear dynamics of hardware-in-the-loop experiments on stickslip phenomena". *International Journal of Non-Linear Mechanics*. in press.
- [2] Budak, E., and Altintas, Y., 1998. "Analytical prediction of chatter stability in milling - part i: General formulation". *ASME Journal of Dynamic Systems, Measurement, and Control*, **120**, Mar., pp. 22–30.
- [3] Insperger, T., and Stepan, G., 2011. *Semi-Discretization for Time-Delay Systems - Stability and Engineering Applications*. Springer, New York.
- [4] Altintas, Y., 2012. *Manufacturing Automation - Metal Cutting Mechanics, Machine Tool Vibrations and CNC Design, Second Edition*. Cambridge University Press, Cambridge.
- [5] Dombovari, Z., Altintas, Y., and Stepan, G., 2010. "The effect of serration on mechanics and stability of milling cutters". *International Journal of Machine Tools and Manufacture*, **50**(6), 6, pp. 511–520.
- [6] Stepan, G., 2001. "Vibrations of machines subjected to digital force control". *International Journal of Solids and Structures*, **38**(10–13), pp. 2149–2159.
- [7] Qin, W. B., and Orosz, G., 2013. "Digital effects and delays in connected vehicles: linear stability and simulations". In Proceedings of the ASME Dynamic Systems and Control Conference, no. DSCC2013–3830, p. V002T30A001.
- [8] Bachrathy, D., and Stepan, G., 2012. "Bisection method in higher dimensions and the efficiency number". *Periodica Polytechnica - Mechanical Engineering*, **56**(2), pp. 81–86.

- [9] Abele, E., Altintas, Y., and Brecher, C., 2010. “Machine tool spindle units”. *{CIRP} Annals - Manufacturing Technology*, **59**(2), pp. 781 – 802.
- [10] Rantatalo, M., Aidanpaa, J.-O., Goransson, B., and Norman, P., 2007. “Milling machine spindle analysis using fem and non-contact spindle excitation and response measurement”. *International Journal of Machine Tools and Manufacture*, **47**(7-8), pp. 1034 – 1045.
- [11] Matsubara, A., Sawamura, R., Asano, K., and Muraki, T., 2014. “Non-contact measurement of dynamic stiffness of rotating spindle”. *Procedia CIRP*, **14**, pp. 484 – 487.
- [12] Matsubara, A., Tsujimoto, S., and Kono, D., 2015. “Evaluation of dynamic stiffness of machine tool spindle by non-contact excitation tests”. *{CIRP} Annals - Manufacturing Technology*, **64**(1), pp. 365 – 368.
- [13] Mancisidor, I., Beudaert, X., Etxebarria, A., Barcena, R., Munoa, J., and Jugo, J., 2015. “Hardware-in-the-loop simulator for stability study in orthogonal cutting”. *Control Engineering Practice*, **44**, pp. 31 – 44.